Environ Geol (2006) 50: 1001–1013
DOI 10.1007/s00254-006-0273-6

ORIGINAL ARTICLE

E. Ferreira da Silva
C. Patinha
P. Reis
E. Cardoso Fonseca
J. X. Matos
J. Barrosinho
J. M. Santos Oliveira

Interaction of acid mine drainage with waters and sediments at the Corona stream, Lousal mine (Iberian Pyrite Belt, Southern Portugal)

Received: 31 January 2006
Accepted: 21 March 2006
Published online: 27 April 2006

E. F. da Silva (✉) · C. Patinha
E. C. Fonseca
Unidade de Investigação ELMAS—Evolução Litosférica e do Meio Ambiental de Superfície,
Departamento de Geociências,
Universidade de Aveiro,
3810-193 Aveiro, Portugal
E-mail: eafsilva@geo.ua.pt

J. X. Matos
Instituto Geológico e Mineiro,
Beja, Portugal
E-mail: joao.matos@ineti.pt

P. Reis
Instituto Superior Técnico,
Avenida Rovisco Pais, Lisboa, Portugal
E-mail: pmarinho@geo.ua.pt

J. Barrosinho
Departamento de Geociências,
Universidade de Aveiro, Aveiro, Portugal

J. M. S. Oliveira
Instituto Geológico e Mineiro,
Porto, Portugal
E-mail: santos.oliveira@ineti.pt

Abstract This study investigates the geochemical characteristics of the acid mine drainage discharged from the abandoned mine adits and tailing piles in the vicinity of the Lousal mine and evaluates the extent of pollution on water and on the stream sediments of the Corona stream. Atmospheric precipitation interacting with sulphide minerals in exposed tailings produces runoff water with pH values as low as 1.9–2.9 and high concentrations of SO_4^{2-} (9,249–20,700 mg l^{-1}), Fe (959–4,830 mg l^{-1}) and Al (136–624 mg l^{-1}). The acidic effluents and mixed stream water carry elevated Cu, Pb, Zn, Cd and As concentrations that exceed the water quality standards. However, the severity of contamination generally decreases 4 km downstream of the source due to mixing with fresh waters, which causes the dilution of dissolved toxic metals and neutralization of acidity. Some natural attenuation of the contaminants also occurs due to the general reduced solubility of most trace metals, which may be removed from solution, by either co-precipitation or adsorption to the iron and aluminium precipitates.

Keywords Acid mine drainage (AMD) · Acidity · Metal ions · Saturation index · Iberian Pyrite Belt, Portugal

Introduction

Sulphide mine waste disposal may constitute an important environmental threat, either in extensively mineralised areas or in localised spot sites. At most mines, some of the metals existing in the mined materials cannot be recovered during mill operations and are discharged into a tailing disposal facility. The mining wastes still containing high metal concentrations represent a source of metal pollution for a long time after extraction. Due to some chemical and geotechnical instability of those materials and due to other potential environmental constraints, this sort of problem can represent long-term public concern. The fragmentation and incoherence of the waste material enhance chemical (oxidation) reactions, particularly

when iron sulphides are present, producing acid mine drainage (AMD). Oxidation of metal sulphides in mines, mine dumps and tailings impoundments originates acidic, metal-rich waters which can contaminate local surface water, groundwater and stream sediments.

AMD has been recognized as a major environmental pollution problem over the past decades (e.g. Letterman and Mitsch 1978; Kleinmann et al. 1981; Gray 1997). AMD as result of the oxidation of minerals containing reduced forms of sulphur [pyrite or its polymorph, marcasite (both FeS_2), pyrrhotite (FeS), galena (PbS), sphalerite (ZnS), chalcopyrite ($FeCuS_2$)] commonly occurs when sulphide bearing minerals in rocks are exposed to air and water, transforming sulphides into sulphuric acid. This means that the more the surface area of rock exposed, the greater the amount of acid. During the mining process, hundreds, sometimes thousands, of tons of rock are dug up and crushed each day. Oxidation of sulphidic mine waste can lead to the discharge of high levels of total dissolved solids (particularly metals and SO_4^{2-}) and low pH waters which can be hazardous to the environment. Certain bacteria, frequently present in these environments, can significantly increase the rate of this reaction. The acid generated leaches and releases heavy metals such as lead, zinc, copper, arsenic, selenium, mercury and cadmium. High concentrations of Fe and Al are also typical in acid sulphate waters (Bigham et al. 1996). Under typical soil conditions, Al activity appears to be controlled by the solubility of gibbsite or kaolinite, while Fe activity is controlled by goethite or amorphous $Fe(OH)_3$ (Nordstrom 1982; Stumm and Morgan 1981). However, in areas of sulphide oxidation, high concentrations of sulphate modify the aqueous geochemistry of Al and Fe. In acid sulphate drainage waters and leachate solutions from mine waste tailings and soils, solubility appears to be controlled by a variety of basic Al/Fe oxides, oxyhydroxides and sulphate phases (goethite, gibbsite, alunite, jurbanite; Karathanasis et al. 1988; Monterroso et al. 1994).

One of the most important problems associated with AMD is water quality degradation, in response to stream acidification due to blow-outs, surface water runoff over tailing piles or erosion of acidic bank side tailings into the creek during thunderstorms. In most of these cases acid drainage can and does occur naturally at specific sites.

The objectives of this study were: (1) to investigate the geochemical characteristics of the AMD discharged from the abandoned mine adits and tailing piles of the Lousal mine, (2) to investigate the mechanisms of dilution and precipitation of some metals in the Corona stream impacted by AMD and (3) to evaluate the polluting extent of AMD.

Description of the study area

The Lousal polymetallic massive sulphide mine is located in the NW region of the Iberian Pyrite Belt (IPB), in a lineament of the volcano-sedimentary complex (VSC) of this volcanic hosted massive sulphides province, which also includes the old Caveira pyrite mine (Fig. 1a).

The Lousal-Caveira VSC lineament is limited to the N by the Grândola fault and by the sediments of the Baixo Sado tertiary basin (BSTB, 1–6 in Fig. 1a), and to the SE by the Alto Sado tertiary basin (ASTB, 7–10 in Fig. 1a) sector of the same sedimentary basin. At W the VSC structure contacts the turbiditic sequences of the Mértola Formation (Baixo Alentejo Flysch Group) by thrust. The Lousal-Caveira VSC lineament is covered by the ASTB overburden in the Alvalade region and it links SE to the Estação de Ourique VSC lineament. The volcanic rocks of the Salgueiral sector (BSTB), intersected by the Sociedade Mineira Rio Artezia boreholes 4 km to the N of the Caveira mine, in the northern block of the Grândola fault, probably represent the NNW continuation of the Lousal-Caveira structure (Oliveira et al. 2001).

In the region of Lousal, the Palaeozoic formations present a NW–SE direction and a SW vergence. The Lousal mine is located in the SW limb of an anticline, which is controlled by N–S and NE–SW late-faults. In the Lousal-Caveira region the following geological units are represented (Strauss 1970; Oliveira et al. 1984; Schermerhorn et al. 1987): phylite–quartzite group (PQG) (Late Devonian)—Corona Fm.—siltitic and carbonated phyllites, siltstones and quartzites; VSC (Upper Famenian–Lower Visean)—black argillaceous shales, volcanoclastics, siliceous shales, graphitic shales, acid metavolcanics, spillites, diabases, jaspers and cherts the host of Lousal massive sulphides; Mértola Fm. (Upper Visean)—turbidites, graywackes, siltstones, shales and conglomerates. The contact between the VSC and the PQG is gradual (Oliveira et al. 1984). In the Lousal sector of the IPB the VSC (Fig. 2) presents the following local units (Silva 1968; Strauss 1970; Matzke 1971): *quartz-keratophire series*: acid volcanoclastics and lavas; *manganese/siliceous shales series*: argillaceous and siliceous shales with spilites and diabases intercalations, jaspers and Mn horizons; *quartz-porphyritic series*: lavas and metavolcanics with quartz phenocrists; *pyrite series*: massive sulphide lenses hosted in black shales with intercalations of volcanoclastics, acid and basic lavas.

The Lousal mining area is limited to the N by the Espinhaço de Cão stream and to the south by the Corona main stream, both tributaries of the Sado river. The geomorphology of the region is controlled at the NW by the Palaeozoic basement of the South Portuguese Zone and at the SE by the tertiary sediments of the ASTB

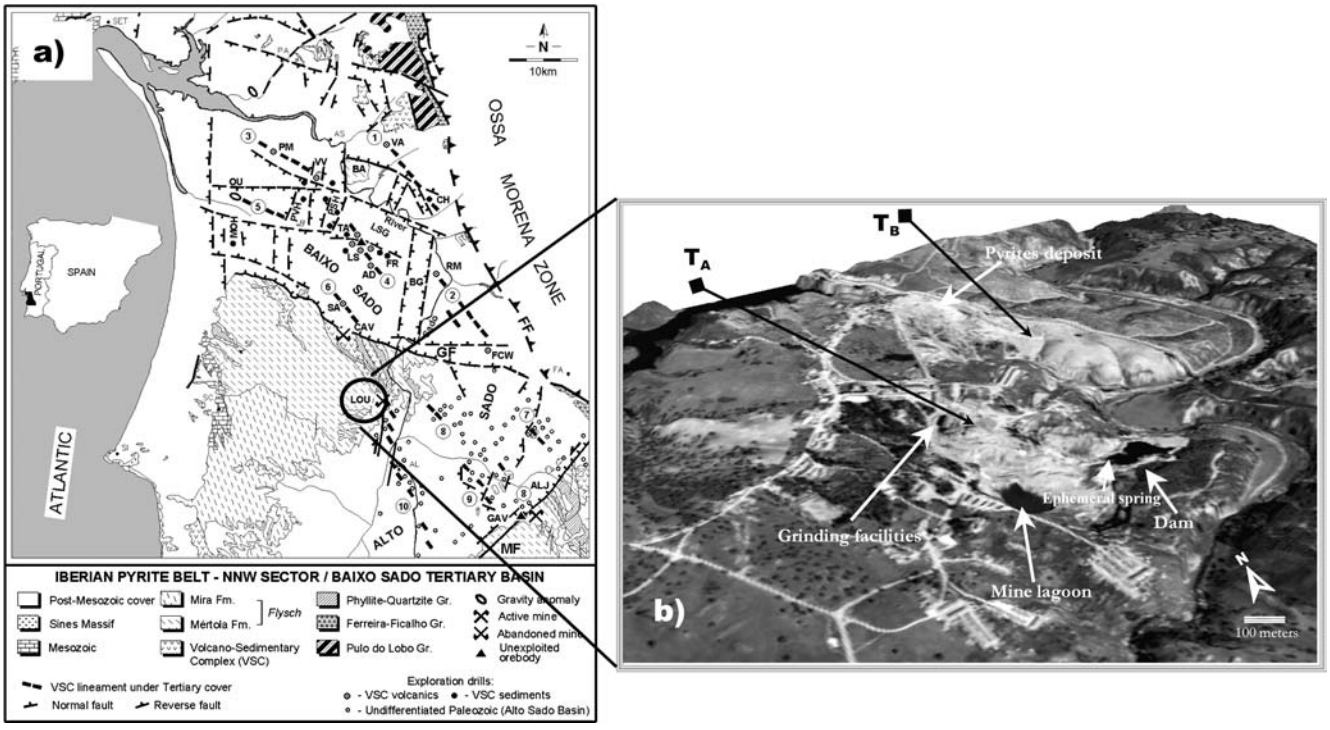

Fig. 1 **a** The NNW sector of the Iberian Pyrite Belt (ad. Oliveira et al. 2001). Baixo Sado VSC lineaments: *1* Vale Água/Chaparral, *2* Rio Moinhos/Fig. Cavaleiros W, *3* Porto Mel—Valverde, *4* Lagoa Salgada/Água Derramada, *5* Outeirão/Pedrogão and *6* Salgueiral. Alto Sado VSC lineaments: *7* Lagoas Paço/Ervidel, *8* Carregueira/Furadouro, *9* Nabos/Milhouros/Aljustrel, *10* Lousal/Alvalade. Main structures: grabens—*BG* Batão, *LSG* L. Salgada NE; horsts—*MOH* Martim Afonso/Outeirão, *PVH* Pedrogão/Valverde, *PSH* Piugada/Mte. Sobral; faults—*GF* Grândola, *MF* Messejana, *FF* Ferreira-Ficalho. Orebodies—*ALJ* Aljustrel, *GAV* Gavião, *LOU* Lousal, *CAV* Caveira, *LS* Lagoa Salgada. **b** Lousal ortophotamap: T_A and T_B tailing piles

(Matzke 1971; Schermerhorn et al. 1987). Close to the principal streams the relief presents a moderate development and the hills have significant slopes.

The ore commonly presents primary banded structures locally with graded grain. The paleogeographic environment of the Lousal deposit is similar to other massive sulphide deposits of the IPB related with black shales like Montinho (Portugal), Tharsis and Sotiel (Spain) (Barriga et al. 1997). The presence of stockwork structures at Lousal opens the possibility, in a first approach, for a metallogenetic system similar to the *brine pool* model defined by Tornos et al. (2000) for Tharsis. Barriga and Carvalho (1983) interpret the presence of sedimentary planar structures on the Lousal ores like the redeposition of pyrite in deeper marine environments. Lousal presents others characteristics similar to Tharsis, which are the presence of carbonated lenses, carbonated ore matrix and the presence of cobalt bearing minerals in the deposits.

Tadeu (1989) in Leistel et al. (1998) estimated for the Lousal mine a total tonnage of 50 Mt, with 0.7% Cu, 0.8% Pb and 1.4% Zn. The massive sulphides are composed predominantly of pyrites (FeS_2) and minor chalcopyrites ($CuFeS_2$), galena (PbS), sphalerite (ZnS), pyrrhotite (FeS), marcasite (FeS_2), bournonite ($CuPbSbS_2$), tetrahedrite ($Cu_{12}Sb_4S_{13}$), arsenopyrite (FeAsS), cobaltite (CoAsS), magnetite (Fe_2O_4) and native gold (Au) (Strauss 1970).

Matzke (1971) presents the following average grades for the Lousal pyrites: Fe 39%; Cu 0.7%; Pb 0.8%; Zn 1.4%; Co 0.08%; Ni 0.01%; S 45%, 0.4%; Sb 0.03%; Mn 0.05%; Sn 0.2%; Cr 0.01%; SiO_2 8.5%; Al_2O_3 1.5%; CaO 0.1%; MgO 0.5%; BaO 0.02%; Au 1g/t. The exploitation method was based on ascending horizontal cuts with posterior fill, being the continuous mining fronts progression maded by a simple inverted step type (Silva 1968). Basic volcanics and argillaceous shales extracted from the surface large open pit were used in the fill process.

The mining significantly altered the morphology of the area. For instance, the material used to fill the abandoned adits was extracted from a quarry that is now collecting water from the flooded adits and wells (due to fluctuations of the water table). This flooded quarry, referred to as the lagoon in Fig. 1b, is about 30 m deep and is blue coloured. The same figure also shows a small dam constructed to retain acid waters draining from the mine, preventing their entrance into the mainstream. This dam is quite shallow, only 2 or 3 m deep, and is full of red coloured water. Nevertheless, the dam shows

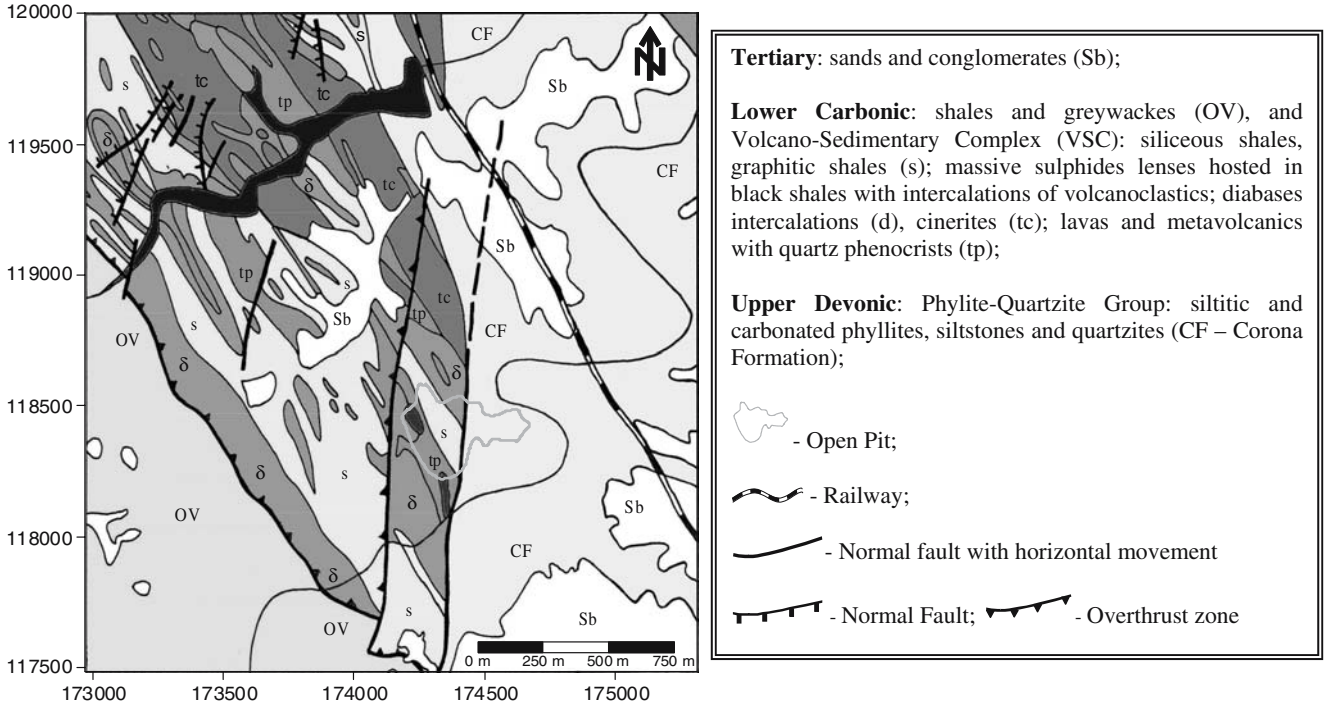

Fig. 2 Geological map of the Lousal sector of the IPB, the volcano-sedimentary complex

punctually some leak at its base resulting in acid water drainage into the mainstream. In the dam, the water level is controlled by the water table rebound and during the wet season this phenomenon is visible at the surface throughout an ephemeral spring. On the small hill, near the railway terminal, a big deposit of fine-grained pyrites remains that was never sent to treatment after the closure of the mine. This deposit is presently covered by soil.

The Lousal mine was exploited basically for pyrite between 1900 and 1988, by surface and underground work to a depth of about 500 m. At the mine the ore was not concentrated within the vicinity of the mine, but it was stored and removed elsewhere for chemical treatment. The only pre-concentration processes used at the site were a previous handmade selection followed by a coarse grinding. The coarse-grained pyrites were then sent to a distant chemical plant to produce sulphuric acid. In the absence of chemical procedures, the potential environmental risk for the site comes mainly from the tailings that have large concentrations of heavy metals (namely lead, arsenic and mercury). The tailings are mostly barren material mixed with the leftovers of the handmade selection. [The volume stored on-site is higher than 1 Mt (Reis et al. 2005; Ferreira da Silva et al. 2005).]

These materials are weakly cemented and consequently the rainwater runoff passing across the tailings causes extensive erosion and transportation of tailing materials into the valley stream. Fieldwork carried out in the Lousal mine revealed that no effective measures were undertaken during mine operation to constrain the tailings erosion and to avoid the generation of AMD. The water flowing downslope from the waste piles represents a potential source of AMD into the Corona stream.

The soils of the region are mostly leptosols, an incipient and lithic soil, and a small area of the soils related with tertiary deposits. These are slightly acid soils, with a sandy texture, very poor in organic matter. The leptosols are acid soils (pH values ranging from 5 to 5.5), poor in organic matter with a very coarse texture. Due to the mining, the soil at the mine itself is now a mixture of soil, rock fragments and tailing material.

The topography of the region is smooth (Fig. 3) and the climate is Mediterranean, dry and warm.

Concerning the use of land in the region, the soils are used mainly for horticulture (orchards) and forestry (eucalyptus). The mining field itself is now in a process of land reclamation through the *Relousal Project*. This project includes a mining museum (now partially open to the public and functioning at the power plant of the mine), and the construction of tourist and cultural facilities, all in the vicinity of the mine (Reis et al. 2005).

Materials and methods

In this study, the selected sample medium consisted of stream sediment, surface water and tailing deposits (T_A and T_B in Fig. 1b).

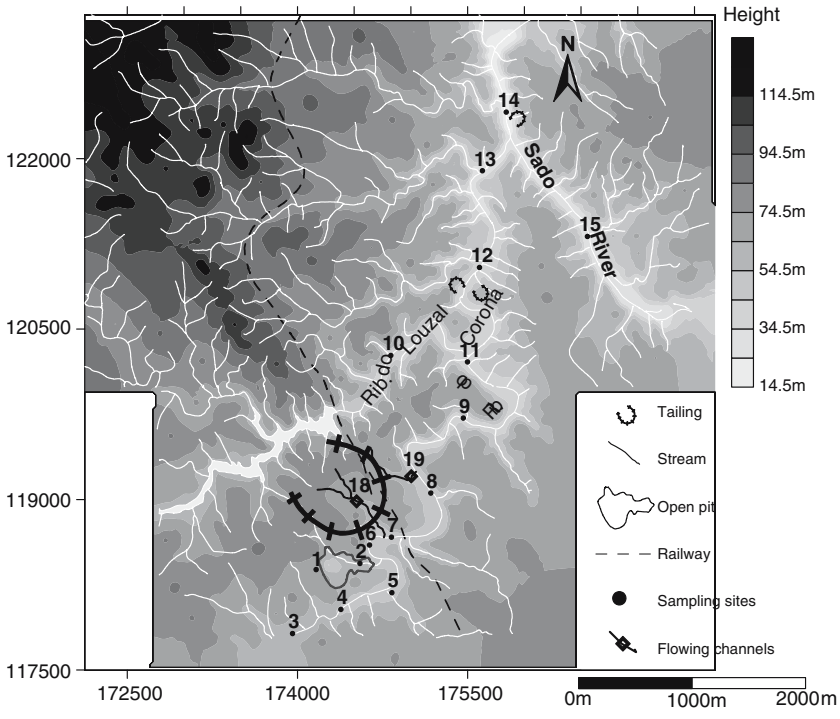

Fig. 3 Map of the Lousal area showing the sampling (surface water and bed-load stream sediment) locations in this study

Surface water samples

Sixteen water samples were collected from streams (samples 3, 4, 5, 6, 7, 8, 11, 12—Corona stream; sample 10—Lousal stream; samples 14 and 15—Sado river), flowing channels emanating from the waste piles (T_A and T_B in Fig. 1b) (samples 18 and 19), lagoons (sample 1) and springs (sample 2), in the study area from February to December 2002. Figure 3 shows the water sampling sites.

Sampling was carried out on each selected site with acid-rinsed polyethylene bottles, and the samples were stored by cooling to 4°C until further analysis.

Values of surface water, pH, temperature and conductivity were determined in the field using a portable HI 8424 microcomputer pH meter calibrated using two Titrisol pH 4 and 7 buffers and a HI 8633 microcomputer conductivity meter.

In order to analyse the dissolved phase, one volume of 250 ml was taken from each sample and filtered on-site through 0.45 μm Millipore membrane filters using an all-plastic pressurized filtering system (ASTM 1984). Analyses of Al, As, Ba, Ca, Cd, Cl, Co, Cr, Cu, Fe, Ga, K, Mg, Mn, Mo, Na, Ni, P, Pb, Sb, Se, Si, Zn, and Cl^- and SO_4^{2-} were carried out. The sample preparation included (1) an acidified, filtered sample for trace and major cation analysis (2) an unacidified, filtered water sample for anion analysis. All of them were kept cool at 4°C prior to laboratory analyses. Samples were acidified to pH < 2 with ultra-pure acid to prevent the precipitation of metals and bacterial growth. Cations and the other trace elements were determined using inductively coupled plasma-mass spectrometry (ICP-MS), whereas the major anions SO_4^{2-} and Cl^- were measured by ion chromatography and HCO_3^- by titration.

Stream sediments and tailing samples

Twelve samples of bed-load stream sediment were collected at water sampling sites whenever sufficient sediment was available (with the exception of sample 11). A total of 22 tailing samples were collected randomly from the T_A and T_B deposits (Fig. 1b).

At the laboratory, tailing and bed-load stream sediment samples were oven dried at a constant temperature of 40°C until a constant weight was attained before dry sieving. Samples were disaggregated and passed through a plastic sieve with a 177 μm aperture. The fine-grained (< 177 μm) fraction of the tailing and stream sediment samples was submitted to a multielemental analysis in an accredited Canadian laboratory (ACME Anal. ISO 9002 Accredited Lab, Canada). A 0.5 g split was leached in hot (95°C) aqua regia (HCl-HNO_3-H_2O) for 1 hour. After dilution to 10 ml with water, the solutions were analysed for 35 chemical elements including Ag, Al, As, Au, Ba, Bi, Ca, Co, Cr, Cu, Fe, Ga, K, La, Mg, Mn, Mo, Na, Ni, P, Pb, S, Sb, Sc, Sr, Th, Ti, U, V and Zn by ICP-atomic emission spectrometry (ICP-ES). In this study, emphasis is given to the following significant chemical parameters: Ag, Al, As, Bi, Cd, Co, Cu, Fe, Mn, Mo, Ni, Pb, Sb, S and Zn.

The analytical precision of the analysis was determined by the analysis of reference materials and duplicate samples (a split of the sample, submitted as two separate samples) in each analytical set.

Powder XRD experiments were performed with a Phillips powder diffractometer, model X'Pert, equipped with an automatic slit. The Cu-X ray tube was operated at 5 kV and 30 mA. Data were collected from 2° to 70° 2θ with a step size of 1° and a counting of 0.6 s.

Results and discussion

Tailing sample

A mineralogical study (XRD) of the tailing samples collected at the A and B areas (Fig. 1b) shows that they are composed of quartz, feldspath, biotite, chlorite, muscovite, illite and kaolinite and also significant proportions of haematite, ilmenite, pyrite, chalcopyrite, galena, sphalerite. The total contents of 35 elements were also determined on these samples. Table 1 shows some statistical parameters, which characterise the relevant elements on environment issues—in this case, Cu, Pb, Zn, As and Cd as hazardous elements and Mn, Fe, S and Al as controllers of the chemical reactions.

The results show that Lousal tailings have high concentrations of Cu, Pb, Zn, As, Cd, Sb, S and Fe, indicating that abundant sulphidic material remains at the A and B sites (Fig. 1b) and is likely to be continuously oxidized for the long-term unless the site is remediated.

The mechanical dispersion downstream and downslope from sites A and B (Fig. 1b) and the metal concentrated acidic waters draining these sites may lead to the contamination of stream sediments and surface waters with As and sulphide-related heavy metals (Cu, Pb, Zn and Cd).

Bed-load stream sediments

Stream sediment samples were submitted to a multielemental analysis. Regarding the three streams that were sampled, the highest values of metal contamination were recorded in the sediments from the Corona stream (Table 2). At the proximal mining areas (mine lagoon and A and B tailings) the sediments are strongly enriched with Fe, S and Al, which can be explained by the large amounts of oxyhydroxide sulphate phases, visible on the stream bed-load and on the fine-grained precipitates deposited at the margins. The concentrations of As, Cu, Pb, Zn and Cd increase by two orders of magnitude relative to the background values measured upstream from the mines (samples 3 and 4) and along adjacent streams that drain unmined areas (sample 10 from the Lousal stream). The concentration strongly decreases downstream from the study area.

Table 1 Characteristics of the statistical parameters of Cu, Pb, Zn, Mn, Fe, As, Cd, Al and S

	n	Average	Median	Minimum	1° Quartile	3° Quartile	Maximum
Cu	36	1,446	934	255	452	1,610	7,013
Pb	36	5,117	5,283	77	2,130	6,696	18,503
Zn	36	1,890	783	126	348	3,115	7,481
Mn	36	131	89	10	26	146	669
Fe	36	21.60	21.88	5.39	9.95	35.37	43.19
As	36	1,450	1,083	386	769	1,575	6,377
Cd	36	3.1	1.4	0.2	0.2	5.7	16.4
Al	36	0.45	0.22	0.01	0.11	0.72	3.24
S	36	16.45	11.24	0.12	2.98	35	47.24

According to Di Toro et al. (1990), stream sediment data provide a useful screening tool for identifying areas that may warrant more costly and time-consuming field toxicity studies. MacDonald et al. (2000) proposed consensus-based stream sediment quality guidelines for 28 metals and organic compounds for freshwater ecosystems. Consensus-based guidelines are based on the criteria previously developed from comparisons of sediment chemistry with toxicity data collected in field studies. Two consensus-based values are reported for each potential contaminant: (1) the threshold effect concentration is the concentration below which harmful effects are unlikely to be observed and (2) the probable effect concentration (PEC) is the concentration above which harmful effects are likely to be observed. In order to assess the quality of the streams at the mining area, total concentrations of As, Cu, Pb, Sb, Zn, Fe, Ag, Ni and Cd were compared to the two consensus-based values proposed by MacDonald et al. (2000).

In the Corona stream, the PEC level is exceeded for As, Cu, Pb, Sb, Zn and Fe in most of the analysed samples (Table 2) and punctually for Ag (sample 7) and Ni (sample 14). Cadmium concentrations never exceed the PEC level.

MacDonald et al. (2000) propose an index allowing the quantification of potential contamination that gives a better perception of the degree of contamination at the site. Using the estimated PEC-Q (sum of all PEC) it is possible to predict the average incidence of toxicity [incidence of toxicity (%) in Table 2] in the impacted stream. The results show that the predicted average incidence of toxicity in the Corona stream ranges from 77 to 100%. Such results reveal that the probability of significant toxicity to infaunal species is extremely high.

Waters

An orientation survey carried out in the area has identified four potential AMD sources entering the Corona stream: mine lagoon (sample 1) collecting water from the

Table 2 Contents of selected elements (Ag, As, Bi, Cd, Co, Cu, Mn, Mo, Ni, Pb, Sb and Zn expressed in mg kg^{-1}; Fe, S and Al expressed in %) in bed-load stream sediments. *TEC* threshold effect concentration, *PEC* probable effect concentration. [a]Distance (m) from the AMD source

Element		Reference Values		Corona stream									Sado river		Lousal stream
				Background		Impacted stream by AMD							Background		
		TEC [b]	PEC [c]	3	4	5	6	7	8	9	11	12	14	15	10
							100[a]	375[a]	1030[a]	2325[a]	3525[a]	4725[a]	5700[a]		
Ag	mg kg^{-1}	1.6	1.9	0.1	0.1	0.2	0.1	15.5	2	0.6	2	2.3	0.3	0.1	0.1
As	mg kg^{-1}	9.79	33	30	8	60	33	1988	704	433	693	654	94	6	25
Bi	mg kg^{-1}	-	-	1.3	1.1	1.8	0.5	89	18.9	6.3	14.5	16.8	3.2	0.6	0.9
Cd	mg kg^{-1}	0.99	4.98	0.2	0.2	3.1	2.3	2.9	0.9	0.4	0.6	0.9	5.7	1.3	0.2
Co	mg kg^{-1}	-	-	11	9	46	27	183	45	17	29	53	73	12	23
Cu	mg kg^{-1}	31.6	149	23	18	171	1986	1060	655	361	485	695	597	94	30
Mn	mg kg^{-1}	460	780	1581	848	2842	459	52	194	118	199	585	4044	655	2147
Mo	mg kg^{-1}	-	-	0.2	0.2	0.6	2	3.6	0.6	0.2	0.6	1.4	0.5	0.2	0.3
Ni	mg kg^{-1}	22.7	48.6	21	19	38	40	10	17	8	17	51	45	15	45
Pb	mg kg^{-1}	35.8	128	99	41	145	85	5891	952	321	808	849	149	17	43
Sb	mg kg^{-1}	2	25	5	1.3	1.8	0.7	173.4	44.1	15.6	41.2	42.2	5.0	0.5	1.3
Zn	mg kg^{-1}	121	459	66	57	1541	1619	1756	600	357	438	657	2398	646	107
Fe	%	2.00	4.00	2.49	1.84	3.5	13.79	27.66	10.09	7.75	10.29	12.56	4.94	1.74	4.84
S	%	-	-	0.06	0.06	0.08	2.22	25.29	6.06	1.79	3.75	4.5	0.76	0.11	0.02
Al	%	-	-	0.93	0.91	1.62	8.22	0.44	0.76	0.56	0.98	1.92	1.87	0.65	1.79
Mean PEC-Q				0,57	0,35	1,40	2,26	15,22	4,20	2,10	3,75	4,12	2,10	0,47	0,68
Incidence of Toxicity (%)				45	31	77	91	100	100	90		100	90		51

Input from lagoon; Tailing; Input Lousal river + tailing; Influence tailing

Table 3 Contents of selected elements in the lagoon, acid spring and flowing channels sample waters

	Lagoon	Acid spring	Flowing channels tailing A	Flowing channels tailing B
pH (–)	2.9–3.0	2.7–2.8	1.9–2.0	2.0–2.3
Cond (μS cm^{-1})	4,635–5,040	4,899–11,610	8,019–20,070	7,530–9,240
SO_4^{2-} (mg l^{-1})	1,546–1,680	1,633–3,870	2,673–6,690	2,510–3,080
Cl (mg l^{-1})	60–151	46–313	1–57	1–19
Ag (μg l^{-1})	0.05–0.54	0.05–0.78	0.3–0.88	0.4–0.11
Al (μg l^{-1})	22,089–26,203	95,477–136,000	624,000–1,100,000	327,000–43,000
As (μg l^{-1})	d.l.	2–95	21,064–36,455	4,574–9,000
Bi (μg l^{-1})	d.l.	0.05–0.15	14,27–26,31	0.05–0.09
Cd (μg l^{-1})	127–181	128–295	180–560	198–300
Co (μg l^{-1})	2,529–3,868	2,109–5,281	1,770–6,499	1,549–3,098
Cu (μg l^{-1})	7,289–10,800	8,864–11,700	23,301–111,000	29,126–49,610
Fe (μg l^{-1})	14,496–22,500	394,706–959,000	2,250,354–8,215,000	1,525,956–1,629,000
Mn (μg l^{-1})	122,089–129,000	101,783–224,036	37,858–49,202	14,316–37,858
Mo (μg l^{-1})	0.3–0.8	0.3–1.3	4.0–9.6	0.1–0.2
Ni (μg l^{-1})	1,082–1,627	1,194–2,007	964–1,349	455–1,349
Pb (μg l^{-1})	143–197	75–306	177–302	d.l.
Sb (μg l^{-1})	d.l.	d.l.	31–130	0.68–1.1
Zn (μg l^{-1})	65,699–77,000	90,461–170,000	199,020–269,000	130,237–219,000

d.l. detection limit (As: 30 μg l^{-1}, Bi: 20 μg l^{-1} and Sb: 10 μg l^{-1})

Table 4 Contents of selected elements in the selected surface water samples. *d.l.* detection limit, *Back* background value, *ND* not determined

			Input water lagoon	Flowing channels					Input Lousal river + tailing	Influence tailing			
			Corona stream									Sado river	Lousal
	Variables		Background		Impacted streamby AMD							Background	
			3	4	5	6	7	8	9	11	12	14	15	10
Winter	pH		7.5	7.4	6,7	7.3	7.2	6.8	6.9	7.3	7.3	7.5	7.6	7.6
	Cond	S cm^{-1}	520	488	464	497	489	511	495	490	503	1365	1384	583
	SO42-	mg l^{-1}	48	41	11	50	56	77	71	66	64	91	91	43
	Cl	mg l^{-1}	44	39	56	39	40	41	40	42	43	157	164	53
	Ag	g l^{-1}	l.d.	l.d.	l.d.	l.d.	l.d.	l.d.	l.d.	l.d.	l.d.	l.d.	l.d.	l.d.
	Al	g l^{-1}	158	188	233	489	617	693	1077	741	685	666	638	31
	As	g l^{-1}	l.d.	l.d.	2	l.d.	2	14	22	9	8	2	l.d	l.d.
	Bi	g l^{-1}	l.d.	l.d.	l.d.	l.d.	l.d.	l.d.	l.d.	l.d.	l.d.	l.d.	l.d.	l.d.
	Cd	g l^{-1}	0.1	l.d.	l.d.	0.3	0.5	1.2	1.0	0.7	0.6	0.5	0.4	l.d.
	Co	g l^{-1}	2	1	1	5	8	14	12	10	9	3	1	l.d.
	Cu	g l^{-1}	6	6	3	14	20	118	108	60	52	21	11	2
	Fe	g l^{-1}	658	642	3541	947	1223	4485	4810	2952	2623	1628	1236	233
	Mn	g l^{-1}	242	219	229	358	450	487	464	428	358	425	342	127
	Mo	g l^{-1}	l.d.	l.d.	l.d.	l.d.	l.d.	l.d.	l.d.	l.d.	l.d.	l.d.	l.d	0.2
	Ni	g l^{-1}	1	l.d.	l.d.	2	3	4	4	4	3	l.d.	l.d	l.d.
	Pb	g l^{-1}	l.d.	l.d.	l.d.	l.d.	3	7	11	7	7	5	l.d	l.d.
	Sb	g l^{-1}	l.d.	l.d.	l.d.	l.d.	0.2	0.5	0.5	0.4	0.3	0.2	0.1	0.2
	Zn	g l^{-1}	60	14	13	218	295	730	615	404	315	277	249	13
Spring	pH		7.26	7.2	6.3	6.4	5.0	3.3	2.8	2.92	3.1	6.0	7.6	7.1
	Cond	S cm^{-1}	870	760	422	930	1025	1240	1621	1363	1284	1173	1041	486
	SO42-	mg l^{-1}	53	43	12	196	398	528	808	526	553	200	78	44
	Cl	mg l^{-1}	174	139	102	152	145	143	131	122	126	226	245	83
	Ag	g l^{-1}	l.d.	l.d.	l.d.	l.d.	l.d.	l.d.	l.d.	l.d.	l.d.	l.d.	l.d.	l.d.
	Al	g l^{-1}	90	69	182	3460	5507	10272	27000	10607	12001	56	97	20
	As	g l^{-1}	l.d.	l.d.	1	l.d.	l.d.	l.d.	5	l.d.	l.d.	l.d.	l.d.	l.d.
	Bi	g l^{-1}	l.d.	l.d.	l.d.	l.d.	0.49	l.d.	l.d.	l.d.	l.d.	l.d.	l.d.	l.d.
	Cd	g l^{-1}	l.d.	l.d.	l.d.	4.8	11.0	17.1	30.1	18.0	19.6	4.1	l.d.	l.d.
	Co	g l^{-1}	2	1	l.d.	95	162	216	321	209	250	64	1	0.2
	Cu	g l^{-1}	5	3	5	225	1206	2219	4717	2607	2903	45	8	4
	Fe	g l^{-1}	853	638	1243	8254	61900	7422	61600	34500	12111	57	192	180
	Mn	g l^{-1}	859	751	132	4144	4323	4514	4609	3529	4298	1373	328	116
	Mo	g l^{-1}	l.d.	l.d.	l.d.	0.2	0.3	l.d.	l.d.	l.d.	l.d.	l.d.	0.2	l.d.
	Ni	g l^{-1}	l.d.	l.d.	l.d.	32	42	51	70	49	56	14	l.d.	l.d.
	Pb	g l^{-1}	l.d.	l.d.	2	3	129	116	492	199	287	l.d.	l.d.	l.d.
	Sb	g l^{-1}	0.1	0.2	l.d.	0.3	5.1	l.d.	0.1	l.d.	l.d.	0.1	0.1	0.1
	Zn	g l^{-1}	33	12	21	2397	4791	7276	12709	7649	8474	2090	55	30
Summer	pH		6.9	7.8	7.4	4,0	2.7	3.4	3.2	4.1	6.6	8.1	8.4	n.d.
	Cond	S cm^{-1}	1179	1030	725	2180	5420	1818	2530	1438	1362	1408	1405	n.d.
	SO42-	mg l^{-1}	24	43	12	1221	4101	1306	728	515	460	131	120	n.d
	Cl	mg l^{-1}	153	139	173	144	178	154	129	122	125	220	241	n.d.
	Ag	g l^{-1}	0.15	0.07	0.25	0.19	0.38	0.29	0.24	0.38	0.36	0.26	0.47	n.d
	Al	g l^{-1}	799	122	583	35409	125000	32000	11361	3045	1013	1515	353	n.d.
	As	g l^{-1}	14	11	13	4	37	4	4	5	13	9	4	n.d
	Bi	g l^{-1}	l.d.	l.d.	l.d.	l.d.	l.d.	l.d.	l.d.	l.d.	l.d.	l.d.	l.d	n.d
	Cd	g l^{-1}	0.9	0.1	0.2	53.4	156.5	49.9	28.6	21.6	2.6	1.0	0.1	n.d
	Co	g l^{-1}	19	3	5	910	2520	774	421	303	48	17	1	n.d
	Cu	g l^{-1}	50	9	16	2446	7623	3128	1955	1018	20	62	17	n.d
	Fe	g l^{-1}	7380	1141	8078	1333	141000	5277	1314	339	1234	1747	554	n.d.
	Mn	g l^{-1}	8325	796	1792	25070	81000	26500	12172	8956	4117	1099	352	n.d
	Mo	g l^{-1}	l.d.	l.d.	l.d.	l.d.	0.5	l.d.	l.d.	l.d.	l.d.	l.d.	l.d	n.d
	Ni	g l^{-1}	5	0.4	2	455	1070	327	181	135	22	3	10	n.d
	Pb	g l^{-1}	3	l.d.	7	22	867	738	198	33	6	11	3	n.d
	Sb	g l^{-1}	0.5	0.6	l.d.	1.9	0.5	0.5	0.5	0.5	2.6	0.1	l.d.	n.d.
	Zn	g l^{-1}	649	73	264	29450	83200	27531	14478	11872	607	719	87	n.d

flooded adits, the ephemeral spring (sample 2) emerging on the dam and two flowing channels (samples 18 and 19) emanating from waste piles (TA and TB). These channels drain directly into the Corona waters whilst the mine lagoon and the spring are not connected with the Corona stream. However, they are connected with

the dam by the water table, which prompted us to study these waters as an AMD source.

The pH of the lagoon water averages 3.0 and the electric conductivity can be as high as 5,040 μS cm^{-1}, although with marked seasonal variations. Trace element concentrations are invariably raised during the dry period. In addition to the high content of SO_4^{2-} and Fe, this water is enriched with Mn, Al, Zn, Cu, Cd and Co (Table 3).

The spring has characteristic acidic water with pH values of 2.8, an electric conductivity as high as 11,610 μS cm^{-1} and high contents of SO_4^{2-}, Fe, Mn, Al, Cd, Co, Cu and Zn.

The flowing channel waters represent a more severe AMD source, in the sense that they have lower pH, higher conductivity and higher contents of SO_4^{2-} and Fe. It is also important to note the extremely high concentrations of Al, As, Cu and Zn.

High concentrations of Fe observed in the spring water and flowing channels (Table 3) are typical of acid sulphate waters emerging as products of the sulphides oxidation, mainly pyrite and also pyrrothite, marcasite, arsenopyrite and chalcopyrite. Sulphuric acid gives the strong acidic property, whereas ferrous hydroxide is responsible for the jelly-like yellowish orange colouration observed in the streambed. The sulphuric acid attacks other sulphide minerals and thus breaks them down to release metals such as Cu, Pb, Zn, Ni, Cd and As. A stronger acid solution increases metal solubility lowering the pH. High concentrations of Al appear to be derived from the weathering of aluminosilicates and from the reaction of the plagioclase occurring in the basaltic rocks, particularly when the pH is low (below 4.5).

The Corona surface waters were collected at stream sediment sampling sites (samples 3, 4, 5, 6, 7, 8, 9, 11, 12). Table 4 shows the physicochemical parameters determined for each sample in three different seasons (winter, spring and summer).

The pH values range from 2.7 to 8.4 depending on season and distance from the sources. pH values steadily increase downstream. The EC as well as concentrations of SO_4^{2-}, Al, Fe, Cu, Ni, Pb, Zn and Mn gradually decrease with increasing distance from the pollution sources. Just as pH values, concentrations of SO_4^{2-}, Al, Fe, Cu, Ni, Pb, Zn and Mn become season dependent.

From an overall analysis of Table 4 two important issues must be stated: (a) during spring the major AMD input to the Corona stream involves the flowing channels emanating from the waste piles confirmed by the lower pH and high heavy metals concentration and (b) during summer the major AMD input comes from the leaky dam.

Considering sample 10 which was collected from the uncontaminated upstream section as a reference sample, the results obtained for the anomalous surface waters show enrichment of Cu 11–1,179 times, Pb 58–248 times, Zn 70–424 times and As 5–611 times above their respective background values (Cu: 4 μg l^{-1}, Pb: 2 μg l^{-1}, Zn: 30 μg l^{-1}, Fe: 180 μg l^{-1}, As: 1 μg l^{-1}, Cd: 0.05 μg l^{-1}, SO_4^{2-}: 15 mg l^{-1} and Al: 20 μg l^{-1}).

In general, high concentrations of Fe, Al and SO_4^{2-} are expected from areas impacted by waste deposits

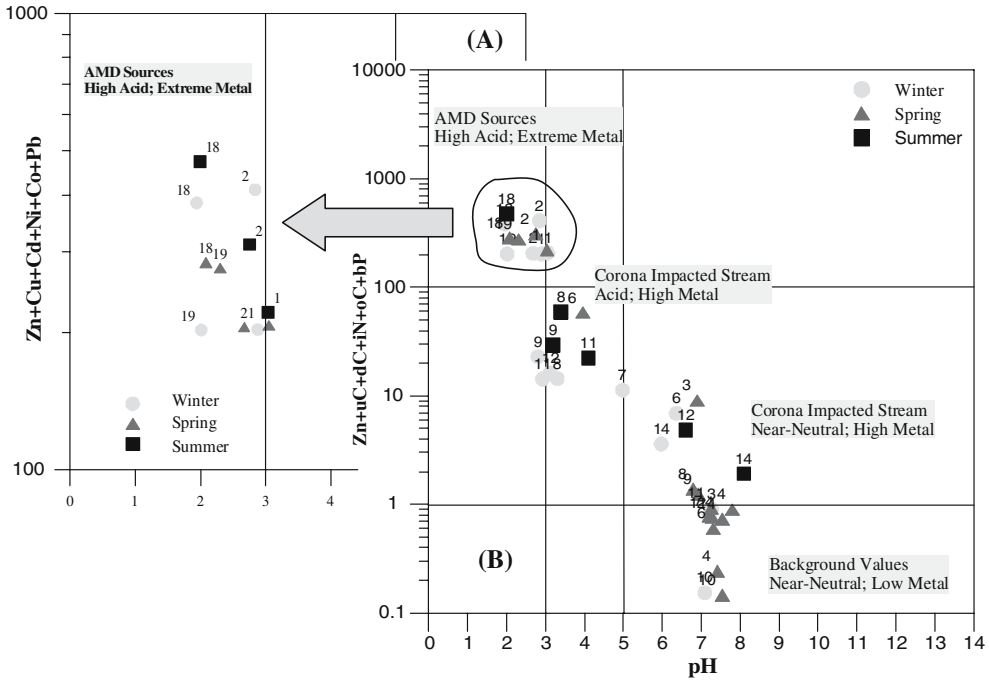

Fig. 4 Ficklin diagrams of pH versus dissolved metal content in water samples collected from the Lousal area. *1* Represents the pond water sample, *2* represents the spring water, *18* and *19* represent the seep waters from the tailing piles, (*6*, *7*, *8*, *9*, *11* and *12*) from the impacted Corona stream, *14* and *15* from the Sado river and *10* from the Lousal stream

Table 5 Calculated saturation indices of iron minerals in stream water calculated using MINTEQ

Site	Corona stream				
Sample number	3	5	8	10	14
pH	7.3	6.3	3.3	7.1	6.0
Saturation index for solid phases Fe					
$Fe(OH)_27ClO_3$	8.15	4.22	−8.66	–	5.07
$Fe(OH)_3$ (ferrihydrite)	3.12	0.51	−9.00	2.29	−0.38
α-FeO(OH) (goethite)	7.09	4.46	−4.86	6.38	3.67
α-Fe_2O_3 (haematite)	19.14	13.86	−4.75	17.74	12.31
FeOOH (lepidocrocite)	6.64	4.03	−5.48	5.81	3.14
Fe_2O_3 (maghemite)	9.63	4.42	−14.61	7.98	2.63
$CuFe_2$ O_2 (cupric ferrite)	15.52	10.30	−13.14	14.00	7.84

derived from the mining activities. High levels of iron and aluminium suggest that these metals remain largely in solution until the Corona reaches the Lousal stream (carrying higher pH water), where mixing causes neutralization and the rapid precipitation of those elements. Further downstream, the pH of the Corona stream increases to values greater than 6.0, together with a decrease in Cu, Pb, Zn, As and Cd concentrations.

Water samples from the studied area were plotted in a diagram developed by Ficklin et al. (1992) (Fig. 4). This plot shows the sum of dissolved base metal concentrations (Cd, Co, Cu, Ni, Pb and Zn) as a function of pH. Data derived from the flowing channel, collected in three different periods, are in the ''high acid/extreme metal'' portion of the Ficklin plot (a), as is shown in Fig. 4. Data from the spring and mine lagoon lie in this same field. The water samples from the impacted Corona stream mainly fall in the ''moderate-acid /high metal'' field (b).

Water–sediment interaction and saturation index

During dry periods, water flowing from the tailings and dam form small ponds dispersed throughout the site. Evaporation of these waters causes co-precipitation of sulphate and metal ions, mainly as melanterite ($FeSO_4.7H_2O$), a pale greenish-blue soluble salt. Beyond melanterite other efflorescent salts occur: rozenite ($FeSO_4.4H_2O$), hexahydrite ($MgSO_4.6H_2O$), epsomite ($MgSO_4.7H_2O$), gypsum ($CaSO_4.2H_2O$). These highly soluble salts represent an instantaneous source of acidic sulphate-rich water upon dissolution and hydrolysis. Hence minerals are important as both sinks and sources of acidity, sulphate and possibly metal ions on precipitation and rapid release on exposure to moisture (Cravotta 1994). The ephemeral nature of most of these minerals (due to their high solubility) makes them difficult to collect (this occurs only during the dry period). Particular salts formed at each site are a function of the local solution composition, pH and relative humidity. According to Jambor et al. (2000) these minerals play an important role in trace cycling between aqueous and solid solutions.

In acid sulphate drainage waters and leachate solutions from mine waste tailings and soils, solubility appears to be controlled by a variety of basic Al/Fe oxides, oxyhydroxides and sulphate phases [goethite, gibbsite, alunite, jurbanite (Karathanasis et al. 1988; Monterroso et al. 1994)]. Studies focused on secondary Fe phases in acid mine waters suggest the presence of the following Fe minerals in the system: $FeOHSO_4$ (Sullivan et al. 1988), α-FeOOH [goethite] (Levy et al. 1997), $KFe_3(SO_4)_2(OH)_6$ [K-jarosite] (Levy et al. 1997), γ-FeOOH [lepidocrocite] (Bigham 1994), $5Fe_2O_3.9H_2O$ [ferrihydrite] (Bigham 1994) and $FeSO_4.7H_2O$ [melanterite] (Monterroso et al. 1994). Bigham (1994) indicates schwertmannite $Fe_8O_8(OH)_6SO_4$ as the most common mineral associated with ochreous precipitates in acidic mine drainage.

An equilibrium mass-balance model has been used to calculate the elemental aqueous speciation and the stability of solid phases with respect to the dissolved constituents. The potential for mineral precipitation or dissolution is assessed using the saturation index (SI) which is based on the relation between analytic activities (the ion activity product observed in solution—IAP) and the theoretical solubility product (K_{sp}). The SI of a mineral is determined using the equation $SI = Log_{10}(IAP/K_{sp})$. If $SI > 0$ the solution is theoretically oversaturated with respect to the solid and precipitation may be expected. For $SI = 0$, the solid and solution are in equilibrium and neither dissolution nor precipitation is predicted to occur. If $SI < 0$, the solution is theoretically undersaturated with respect to the solid if present in the system and dissolution might be possible.

Geochemical modelling, using the equilibrium computer code PHREEQC (Parkhurst 1995) and the MINTEQ database (Allison et al. 1991), was performed to calculate the SIs.

Physical conditions and elemental concentrations of surface waters from the Corona and Lousal streams (samples 3, 5, 8, 10 and 14) were used as input data to the computer modelling.

Table 5 shows the expected species of Fe in each selected water sample. The results show that, with the exception of sample 8, all water samples are oversaturated with respect to the solid. In these conditions precipitation of goethite, haematite, lepidicrocite and maghemite may be expected. The SI for ferrihydrite is positive and is > 1 for samples 3 and 10. Ferrihydrite is likely to form in slightly acid–alkaline solutions (samples 3 and 10) with very high levels of dissolved Fe (Bigham 1994). Langmuir and Whittemor (1971) suggest that $Fe(OH)_3$ and poorly crystalline goethite are the first ferric phases to precipitate in streams impacted by acid mine waters, although they will pass to the more stable phases with time, crystalline goethite and lepidocrocite.

Lepidocrocite is the major initial product of oxidation and precipitation of the ferrous iron bearing solution, although the presence of other metal ions plays a role in determining crystallinity and stability towards goethite (Schum and Lavkulich 1999).

Summary and conclusions

The survey at the Lousal area included the sampling of tailings, stream sediments, stream waters and various acid soluble metal phases that precipitate during the dry season.

On tailings, the total concentrations of metals and metalloids were determined by ICP-MS as well as a mineralogical study by XRD to identify the major mineral phases. The results show that the Lousal tailings have high concentrations of Cu, Pb, Zn, As, Cd, Sb, S and Fe indicating that abundant sulphidic material remains at the A and B sites.

Regarding the stream sediments and similar to the tailings, the total concentrations of metals and metalloids were determined by ICP-MS. For these media, we use some contamination criteria to assess exceeding levels, which enable the use of PEC-Q to predict toxicity. The results show that stream sediments immediately downstream of the AMD sources show high metal concentrations. The concentrations increase several orders of magnitude relative to the background values measured upstream from the mine. This increase is related to the mechanical dispersion of the pyritic material from the tailings. Also, the exposure of this material to air and water promotes acid generation and metal mobility in surface runoff. The PEC-Q predicted, at the Corona River, an average incidence of toxicity of $\sim$ 89%, meaning that the exposure to faunal species is a possibility.

For water samples, we determined some physical and chemical parameters, like pH, electric conductivity and total element concentrations. The variation of these parameters was assessed through a spatio-temporal interpretation of the tables. Such methodology allowed the identification of 4 major AMD inputs into the Corona stream: two flowing channels emanating from the waste piles, the mine lagoon and the ephemeral spring.

Values for pH, EC and trace metal concentrations significantly vary in the surface water of the Corona stream since season and surface water conditions are important controlling factors for these parameters.

During spring, the major AMD input to the Corona stream is the flowing channels emanating from the waste piles and during summer the leaky dam.

The acidity of the AMD is buffered to a greater or lesser degree by dilution from the drainage network of the Corona stream; yet the water still contains considerable amounts of metals (approximately 4 km downstream).

To understand the processes occurring at the sediment–water interface, we performed a chemical and mineralogical characterization of the acid soluble metal-phases that precipitate during the dry season. The results show that such phases are mostly acid inorganic metal bearing phases as melanterite, rozenite, hexahydrite, epsomite and gypsum, and secondary Al/Fe oxides, oxyhydroxides and sulphates (ochre precipitates). The dissolution of these secondary minerals during storm events can dramatically alter the chemistry of surface water with significant short-term effects. However, during the dry season, the precipitation of secondary minerals and sorption of metals onto ochre minerals improve water quality by removing heavy metals from the solution. However, these minerals become part of the sediment where they may impact benthic organisms since sediment samples in the studied area exceed threshold quality guidelines for aquatic systems.

Nevertheless, this process is important in metal cycling and acidity between solids and solutions in surface environments.

Related to the proposal for remediation of the Lousal area the former owner and the local council jointly devised an integrated development program with a cultural component that should reclaim Lousal economically and socially. The former mine owner and the local council were brought together in the Frédéric Velge Foundation the Lousal Integrated Development and Revitalisation Program (RELOUSAL Program). Based on this program the majority of the abandoned mining buildings and industrial equipment will be reclaimed. This program includes the building of tourist facilities (small hotels, restaurants, leisure facilities, a campsite and opportunities for rural tourism) as well as vocational training.

Due to the spatial extensiveness of the contaminated area only the tailing deposits and the contaminated sediments/alluvium from the Corona stream must be excavated and shipped off-site to landfill. This landfill could be installed inside the open pit. However, this option may be expensive as the price is by the ton. Another approach is the consolidation of waste piles in order to reduce water quality impacts. More than 1 Mt of contaminated soils, sediments and mine processing wastes must be consolidated on-site. The re-grading of the area will prevent erosion by reducing water runoff and will provide a more stable surface.

Once consolidated, a variety of measures must be taken including diversion trenches and culverts, evaporation ponds and capping (impermeable layer and soil) in order to minimize contaminated runoff leaving the site. The capping idea is that the remaining solid material, high in metals and/or acid-producing material, will not be exposed to superficial weathering. According to Costello (2003) this solution is a reasonable option for reducing hazard to potential receptors (risks associated

with dermal contact and/or incidental ingestion of surface soils) but they generally do not reduce the toxicity or volume of the metals present in the soil. Revegetation with seeds is needed to reinforce the topsoil, to reduce soil erosion and runoff velocity and to remove water from the soil by evaporation.

Related to the water resources, the flooded adits are an important source of pollution. The major concern is the water table rebound, responsible for the formation of the dam of acidic waters and the ephemeral spring draining directly to the Corona stream. The underground connection between the abandoned adits and wells, the dam and the ephemeral spring, makes this a complex system of ''diffuse'' sources of AMD. To solve this complex problem of AMD we propose a wetland system, located between the groundwater spring and the Corona stream. This system should be composed of two different sections, one with an aerobic environment used basically for iron precipitation and another with an anaerobic environment for the precipitation of heavy metals.

With this approach the inputs of contaminant loadings to the Corona stream are restricted, water quality is maintained on an acceptable level and the accumulation of contaminated sediments is avoided.

Acknowledgments This study was made possible with the financial support provided by IAPMEI (Instituto de Apoio ás Pequenas e Médias Empresas e ao Investimento – Ministério da Economia). Particular acknowledgments are addressed to Instituto Geológico e Mineiro (presently INETI Inovação) for authorizing the use and the publishing of the geochemical and hydrochemical data from the Project ''Estudo do Controle Ambiental nas áreas mineiras abandonadas de Lousal e Caveira). The anonymous reviewers are thanked for their comments and suggestions on the manuscript, which helped to improve this paper.

References

Allison JD, Brown DS, Novo-Gradac KJ (1991) MINTEQA2/PRODEFA2: a geochemical assessment model for environmental systems, version 3.0. User's Manual, Environmental Research Laboratory, Office of Research and Development, U.S. Environmental Protection Agency, EPA/600/3-91/021, Athens, Georgia, 30605, p 92

ASTM (1984) American Society for Testing Materials, Annual Book of ASTM Standards. Water Environmental Technology, vol 11.01

Barriga FJAS, Carvalho D (1983) Carboniferous volcanogenic sulphide mineralization in south Portugal (Iberian Pyrite Belt), Mem. SGP, no. 29, pp 99–113

Barriga FJAS, Carvalho D, Ribeiro A (1997) Introdution to the Iberian Pyrite Belt. SEG Neves Field

Bigham JM (1994) Mireralogy of ochre deposits formed by sulphide oxidation (Chap. 4). In: Jambor JL, Blowes DW (eds) Environmental geochemistry of sulphide mine-wastes, short course handbook. Mineralogical Society of Canada, vol 22. Waterloo, Ontario, pp 103–132

Bigham JM, Schwertmann U, Traina SJ, Winland RL, Wolf M, (1996) Schwertmannite and the chemicalmodeling of iron in acid surface waters. Geochem Cosmochem Acta 60:2111–2121

Costello C (2003) Acid mine drainage: innovative treatment technologies National Network of Environmental Studies Fellows. US Environmental Protection Agency, Washington, 52 pp

Cravotta CA (1994) Secondary iron-sulfate minerals as source of sulfate and acidity. In: Alpers CM, Blowes DW (eds) Environmental geochemistry of sulfide oxidation. American Chemical Society Symposium Series 550, Washington, pp 345–364

Di Toro DM, Mahoney JD, Scott KJ, Hicks JB, Mays SM, Redmond MS (1990) Toxicity of cadmium in sediments-the role of acid-volatile sulphide. Environ Toxicol Chem 9:1487–1502

Ferreira da Silva E, Cardoso Fonseca E, Matos JX, Patinha C, Reis P, Santos Oliveira JM (2005) The effect of unconfined mine tailings on the geochemistry of soils, sediments and surface waters of the lousal area (Iberian Pyrite Belt, Southern Portugal). Land Degrad Develop 16:213–228

Ficklin WH, Plumlee GS, McHugh JB (1992) Geochemical classification of mine drainages and natural drainages in mineralized areas. In: Proceedings of the 7th international symposium on water–rock interaction, Park City, Utah

Gray NF (1997) Environmental impact and remediation of acid-mine drainage: a management problem. Environ Geol 30:62–71

Jambor JL, Nordstrom DK, Alpers CN (2000) Metal-sulfates salts from sulphide mineral oxidation. In: Alpers CN, Jambor JL, Nordstrom DK (eds) Sulfate minerals—crystallography, geochemistry, and environmental significance. Rev Mineral 40:303–350

Karathanasis AD, Evangelou VP, Thompson YL (1988) Aluminium and iron equilibria in soil solutions and surface waters of acid mine watersheds. J Environ Qual 17:534–543

Kleinmann RLP, Crerar DA, Pacelli RR (1981) Biogeochemistryof acid mine drainage and a method to control acid formation. Min Eng 33:300–304

Langmuir D, Whittemor DO (1971) Variations in the stability of precipitated ferric oxyhydroxides. In: Hem JD (ed) Nonequilibrium systems in natural waters chemistry. Adv Chem Ser 106:209–234

Leistel J, Marcoux E, Thiéblemont D, Quesada C, Sánchez A, Almodóvar G, Pascual E, Sáez R (1998) The volcanic-hosted massive sulphide deposits of Iberian Pyrite Belt. Mineralium Deposita 33:2–30

Letterman RD, Mitsch WJ (1978) Impact of mine drainage on a mountain in Pensylvania. Environ Pollut 17:53–73

Levy DB, Custis KH, Casey WH, Rock PA (1997) The aqueous geochemistry of the abandoned Spenceville Copper Pit, Nevada Country, California. J Environ Qual 26:233–243

MacDonald DD, Ingersoll CG, Berger TA (2000) Development and evaluation of consensus-based sediment quality guidelines for freshwater ecosystems. Arch Environ Contam Toxicol 39:20–31

Matzke, K (1971) Mina do Lousal. Principais Jazigos Minerais do Sul de Portugal. Liv-Guia 4:25–32

Monterroso C, Alvarez E, Macías F (1994) Speciation and solubility controls of Al and Fe in minesoil solutions. Sci Total Environ 158:31–43

Nordstrom DK (1982) Aqueous pyrite oxidation and the consequent formation of secondary iron minerals. In: Kittrick JA, Fanning DS, Hossner LR (eds) Acid sulphate weathering. Proceedings of a symposium sponsored by Divisions S-9, S-2; S-5, and S-6 of the Soil Science Society of America in Fort Colins, 5–10 August 1979 (SSSA special publ. no. 10) Colorado, pp 37–56

Oliveira JT et al (1984) Carta Geológica de Portugal 1/200000, Notícia Explicativa Fl. 7 SGP

Oliveira VMJ, Matos JX, Rosa C (2001) The NNW sector of the Iberian Pyrite Belt—new exploration perspectives for the next decade. Geode Workshop —massive sulphide deposits in the Iberian Pyrite Belt: new advances and comparison with equivalent systems, Aracena, Spain, pp 34–37

Parkhurst DL (1995) Users guide to PHREEQC: a computer model for speciation, reaction-path, advective transport and inverse geochemical calculations, U.S. Geological Survey, Water-Resources Investigations, Report 95–4227

Reis AP, Ferreira da Silva E, Sousa AJ, Matos J, Patinha C, Abenta J, Cardoso Fonseca E (2005) Combining GIS and stochastic simulation to estimate spatial patterns of variation for lead at the lousal mine, Portugal. Land Degrad Develop 16:229–242

Schermerhorn L, Zbyzewski G, Ferreira V (1987) Carta Geol. Portugal 1/50000 42D Aljustrel, SGP, p 55

Schum M, Lavkulich L (1999) Speciation and solubility relationship of Al, Cu, and Fe in solutions associated with sulphuric acid leached mine waste rock. In: Environmental geology, vol 38, no. 1. Springer, Berlin Heidelberg New York, pp 59–68

Silva F (1968) As Minas do Lousal. Bol. Minas, Dir. Geral de Minas e SGP, 5 (3), pp 161–181

Strauss G (1970) Sobre la geologia de la provincia piritífera del SW de la Península Ibérica y de sus yacimientos, en especial sobre la mina de pirita de Lousal (Portugal). Mem. ITGE T. 77, pp 266

Stumm W, Morgan JJ (1981) Aquatic chemistry: an introduction emphasizing chemical equilibria in natural waters. New York, Wiley

Sullivan PJ, Yelton JL, Reddy KJ (1988) Solubility relationships of aluminium and iron minerals associated with acid mine drainage. Environ Geol Water Sci 11:283–287

Tornos F, Barriga F, Marcoux E, Pascual E, Pons JM, Relvas J, Velasco F (2000) The Iberian Pyrite Belt. Database on global VMS districts. In: Large R, Blundell D (eds) CODES SRC, Tasmania, pp 19–52